

REPORT DOCUMENTATION PAGE				Form Approved OMB No. 0704-0188	
Public reporting burden for this collection of information is estimated to average 1 hour per response, including the time for reviewing instructions, searching existing data sources, gathering and maintaining the data needed, and completing and reviewing this collection of information. Send comments regarding this burden estimate or any other aspect of this collection of information, including suggestions for reducing this burden to Department of Defense, Washington Headquarters Services, Directorate for Information Operations and Reports (0704-0188), 1215 Jefferson Davis Highway, Suite 1204, Arlington, VA 22202-4302. Respondents should be aware that notwithstanding any other provision of law, no person shall be subject to any penalty for failing to comply with a collection of information if it does not display a currently valid OMB control number. <b>PLEASE DO NOT RETURN YOUR FORM TO THE ABOVE ADDRESS.</b>					
1. REPORT DATE (DD-MM-YYYY) 12/01/2011		2. REPORT TYPE Technical Paper		3. DATES COVERED (From - To) 2011	
4. TITLE AND SUBTITLE  Dielectric Nonlinear Transmission Line (POSTPRINT)				5a. CONTRACT NUMBER FA9451-08-D-0170/0013	
				5b. GRANT NUMBER	
				5c. PROGRAM ELEMENT NUMBER	
6. AUTHOR(S)  David M. French, Brad W. Hoff, Susan Heidger, Don Shiffler				5d. PROJECT NUMBER	
				5e. TASK NUMBER D00M	
				5f. WORK UNIT NUMBER PPM00001467 DF702136	
7. PERFORMING ORGANIZATION NAME(S) AND ADDRESS(ES) Air Force Research Laboratory 3550 Aberdeen Avenue SE Kirtland AFB, NM 87117-5776				8. PERFORMING ORGANIZATION REPORT NUMBER	
9. SPONSORING / MONITORING AGENCY NAME(S) AND ADDRESS(ES)  Air Force Research Laboratory 3550 Aberdeen Avenue SE Kirtland AFB, NM 87117-5776				10. SPONSOR/MONITOR'S ACRONYM(S) AFRL/RDHP	
				11. SPONSOR/MONITOR'S REPORT NUMBER(S)  AFRL-RD-PS-TP-2012-0004	
12. DISTRIBUTION / AVAILABILITY STATEMENT Approved for public release; distribution limited.					
13. SUPPLEMENTARY NOTES 377ABW-2011-1186; 11 August 2011 Published in the 2011 IEEE Pulsed Power Conference Proceedings, 01 December 2011. Government Purpose Rights.					
14. ABSTRACT A parallel plate nonlinear transmission line (NLTL) was constructed. Periodic loading of nonlinear dielectric slabs provides the nonlinear capacitance and the gaps between provide linear inductive interconnects, this is essentially the same design used by Ikezi [1],[2]. The NLTL was modeled in a circuit simulation code using the experimentally measured form of the nonlinear capacitance. Dielectric loss included in the model as an equivalent series resistance derived from the measured loss tangent data affects the formation of RF oscillations. The diagnostics used on the experimental system are Bdots along the line and a current viewing resistor at the load. The diagnostics provide a measurement of the pulse evolution as it travels down the line. The waveforms from the experimental line qualitatively agree with the circuit model, showing no strong RF formation as a result of the loss.					
15. SUBJECT TERMS					
16. SECURITY CLASSIFICATION OF:			17. LIMITATION OF ABSTRACT  SAR	18. NUMBER OF PAGES  6	19a. NAME OF RESPONSIBLE PERSON David French
a. REPORT UNCLASS	b. ABSTRACT UNCLASS	c. THIS PAGE UNCLASS			19b. TELEPHONE NUMBER (include area code) 505-846-9101

# Dielectric Nonlinear Transmission Line

David M. French, Brad W. Hoff, Susan Heidger, Don Shiffler

Directed Energy Directorate  
Air Force Research Laboratory, Kirtland AFB, NM

## Abstract

A parallel plate nonlinear transmission line (NLTL) was constructed. Periodic loading of nonlinear dielectric slabs provides the nonlinear capacitance and the gaps between provide linear inductive interconnects, this is essentially the same design used by Ikezi [1],[2]. The NLTL was modeled in a circuit simulation code using the experimentally measured form of the nonlinear capacitance. Dielectric loss included in the model as an equivalent series resistance derived from the measured loss tangent data affects the formation of RF oscillations. The diagnostics used on the experimental system are Bdots along the line and a current viewing resistor at the load. The diagnostics provide a measurement of the pulse evolution as it travels down the line. The waveforms from the experimental line qualitatively agree with the circuit model, showing no strong RF formation as a result of the loss.

## Introduction

A nonlinear transmission line (NLTL) was constructed in a parallel plate design, using nonlinear dielectric slabs as the nonlinear medium. The NLTL uses 50 parallel plate L-C sections spaced evenly along the length of the transmission line. Each L-C section is comprised of a parallel plate region loaded with a nonlinear dielectric slab followed by an unloaded section which was filled with transformer oil in the experiment, Figure 1. The dielectric slabs provide a nonlinear capacitance, and the gaps between provide linear inductive interconnects. In the basic circuit model used for this configuration the L and C values for a given stage are determined by calculating the L and C values of the capacitor region and inductor region and summing the two. The nonlinear dielectric material

used for the capacitor regions was a lead-manganese-niobate ceramic made by the TRS company, designated PMN38 [3].

**Table 1. Circuit parameters for NLTL with PMN38 capacitors.**

Zero Voltage		Saturated	
<b>L (nH)</b>	13.2	<b>L (nH)</b>	13.2
<b>C (pF)</b>	170	<b>C (pF)</b>	50
<b>f (MHz)</b>	106	<b>f (MHz)</b>	196
<b>Z (<math>\Omega</math>)</b>	8.8	<b>Z (<math>\Omega</math>)</b>	16.2

The zero voltage capacitance of the PMN38 capacitors used for this NLTL is 170pF. An estimate of the per stage inductance (L) and capacitance (C) in transformer oil ( $\epsilon = 2.2$ ), based on geometric calculations, is summarized in Table 1, which also includes the characteristic frequency,  $f = 1/2\pi(LC)^{1/2}$ , and impedance,  $Z = (L/C)^{1/2}$ .

## Transmission line construction

The transmission line was built using two brass plates that have channels milled to index the capacitor location, shown in Figure 1. The dielectric slab dimensions are 1.5x15x20 mm with the 1.5x15 mm faces metalized so that they can be epoxied to the brass plates. The capacitors and brass plates were cleaned with alcohol before the dielectric slabs were bonded to the plates with conductive epoxy. Because the resistivity of the epoxy depends upon the temperature at which it is cured, after epoxy application the assembled line was clamped together with metal clamps and baked at 105° C at a pressure of less than 100  $\mu$ Torr for 24 hours. After baking, the assembled line was quickly transferred to a plastic clamping assembly and placed under oil to minimize the time the clean and dry NLTL spent in moist ambient air. This is an important consideration as

any surface contamination on the capacitors may lead to increased likelihood of surface tracking when high voltage is applied to the transmission line.

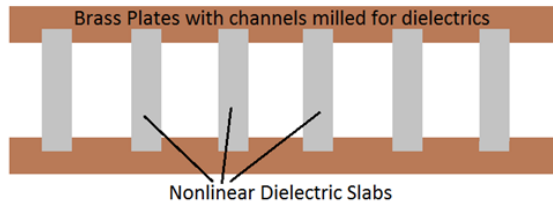


**Figure 1. Parallel plate transmission line using the Ikezi geometry.**

## Transmission Line Driver

The transmission line was driven by a sparkgap switched 6.25  $\Omega$  Blumlein pulse forming line that generates ~50 ns square pulses with ~6 ns rise and fall times at up to 50 kV. The output of the pulser is connected to eight 50  $\Omega$  cables that attach to the input of the NLTL.

## Capacitor modeling

The capacitance-voltage characteristic is modeled by a Lorentzian that was fit to the measured dielectric constant data and scaled to the capacitance of the slabs. LTspice [4] has a nonlinear capacitance model that uses the functional form of the charge to determine the current and voltage on circuit elements. The function  $C(V)$  is plotted in Figure 2 up to 20 kV, the highest voltage for which measured data were available.

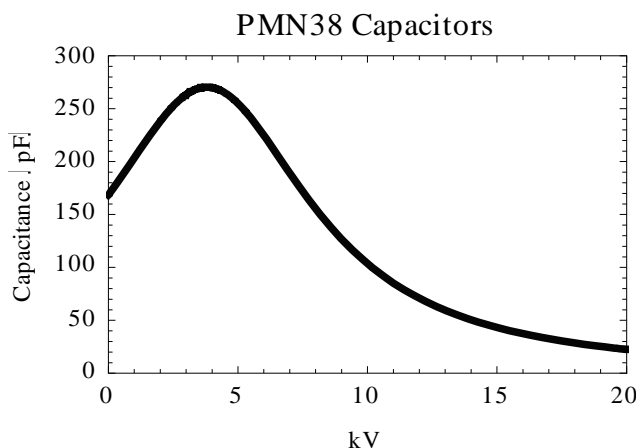


**Figure 2. Capacitance function that is used in the LTspice circuit models.**

In order to verify that the simulation is using the correct model of the capacitance, a simple test is

performed on a single capacitor as a pulse moves down the transmission line. The current through the capacitor is  $I = dq/dt$ , the finite difference current is  $I_n = \Delta q_n / \Delta t_n$ . The change in charge  $\Delta q_n$  at time  $t_n$  can be calculated by taking the current  $I_n$  and multiplying by the timestep  $\Delta t_n = t_n - t_{n-1}$ . The change in charge  $\Delta q_n$  can be divided by the change in voltage,  $\Delta V = V_n - V_{n-1}$  to get the capacitance-voltage relationship  $C(V) = \Delta q_n / \Delta V_n$  at voltage  $V_n$ . This test of the capacitance in the code assures that the model is correctly simulating the experimental capacitors.

## Circuit Simulations

Using the functional form of the capacitance and the analytically determined per stage inductance, the 50 stage NLTL circuit is modeled in LTspice [4].

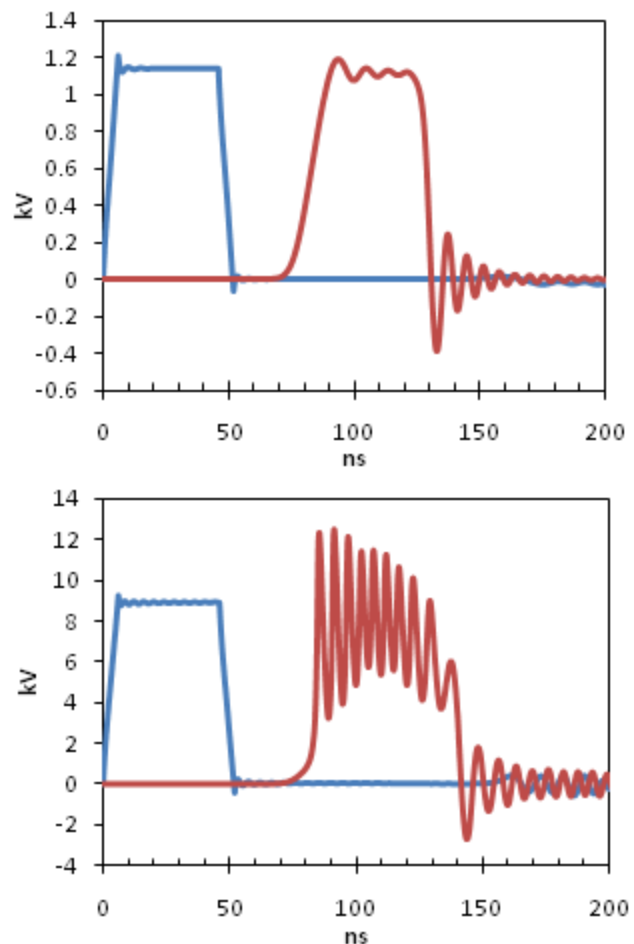


**Figure 3. Input (blue) and output (red) traces showing the behavior of the simulated lossless 50 stage NLTL using the PMN38 capacitance.**

The pulser is modeled as a  $6.25\ \Omega$  source that puts out a 50 ns wide pulse with 6 ns rise and fall times. The NLTL is terminated in a  $13\ \Omega$  coaxial load with a total output inductance of  $\sim 50\ \text{nH}$ . Figure 3 shows the behavior of a lossless 50 stage NLTL circuit for different voltage of the input pulses. At input voltages below that corresponding to peak capacitance ( $\sim 4\ \text{kV}$ ) the risetime of the pulse is increased because the lower voltage portion of the pulse travels faster than the peak, effectively stretching the pulse in time and increasing the time to peak. The same effect results in an electromagnetic shockwave being formed at the fall of the pulse. Following the electromagnetic shock at the end of the pulse, oscillations about zero voltage are observed. This effect can be used for pulse sharpening and RF generation about 0 volts with dielectrics or capacitors with positive  $dC/dV$ . When the peak voltage of the input pulse is above the 4 kV threshold,  $dC/dV$  becomes negative, therefore a shock will be formed at the rise of the pulse. The bottom pane of Figure 3 shows a 9 kV input pulse and the resulting output pulse which displays oscillations after the rise of the pulse. In the experimental line, dielectric loss will dissipate energy from the RF wave. In order to more accurately model the experiment loss must be included in the calculations.

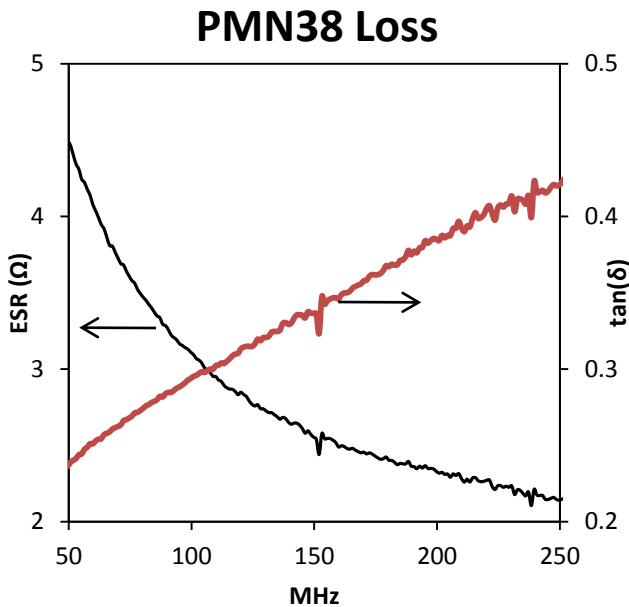


Figure 4. PMN38 loss tangent as a function of frequency, measured at zero voltage and equivalent series resistance for the capacitors used in the experiment.

## Loss Considerations

The loss of a capacitor is typically given as the loss tangent,  $\tan\delta$ . The circuit model of a real capacitor is an ideal capacitor of capacitance  $C$  and an equivalent series resistance of resistance  $\text{ESR}$ . The loss tangent is expressed as  $\tan\delta = \omega C \cdot \text{ESR}$ , where  $\text{ESR}$  is the equivalent series resistance of the capacitor, and  $\delta$  is the angle between the complex and real parts of the impedance. The PMN38 material loss tangent data taken at zero voltage are shown in Figure 4. Using the loss tangent data, the equivalent series resistance as a function frequency can be determined, Figure 4. An equivalent series resistance is put into the LTspice model to take into account the loss that will be present. In order to include dielectric loss effects in the circuit simulations, the  $\text{ESR}$  for a single frequency is put into the model in series with the lossless capacitors. To determine the specific  $\text{ESR}$  value to be used, a simulation is first run without resistive loss in order to determine the center frequency of oscillation. The  $\text{ESR}$  for this center frequency is then added to subsequent simulations.

### 50 stage PMN38 NLTL

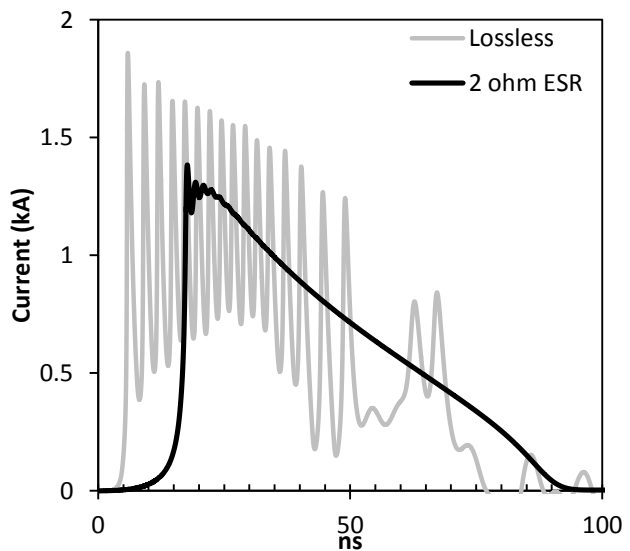


Figure 5. Output of 50 stage NLTL showing lossless case and  $2\ \Omega$  ESR case.

Although there are a very broad range of frequencies present in the NLTL waveform, this method will provide approximately the correct damping at the dominant frequency of oscillation. Including the dielectric losses of the PNM38 in the model allows estimation of the severity of the

damping experienced by the RF oscillations. In cases of excessive damping, no RF will be observable at the output of the transmission line. From Figure 4 it is clear that the ESR is at least  $2\ \Omega$  for the PMN38 material at the frequencies of interest. Circuit simulations comparing the lossless and  $2\ \Omega$  ESR are shown in Figure 5. The  $2\ \Omega$  NLTL waveform is approximately what is expected from the experimental line as the model includes the correct form of the capacitance, inductance, and loss.

## Experimental Diagnostics

The diagnostics used on the experimental system are Bdot sensors along the line and a commercial 1.2 GHz bandwidth current viewing resistor (CVR) at the load. The CVR was used as a reference in order to calibrate the Bdot probes in the transmission line prior to installing the capacitors as well as providing the exit current at the termination of the NLTL. Four sets of Bdot probes were spaced along the NLTL. Each Bdot set was comprised of 4 probes inserted in adjacent stages for a total of 16 Bdots. The first Bdot set monitored stages 0-3, the second set monitored stages 10-13, the third set monitored stages 25-28, and the fourth set monitored stages 40-43. The entrance current was measured with Bdot zero and the exit current is measured with the CVR. The diagnostics are visible in Figure 6. The calibration of the Bdot probes was performed by pulsing the line prior to installing the dielectric slabs, the Bdot probe traces were then integrated and calibrated with the reference current from the commercial CVR.

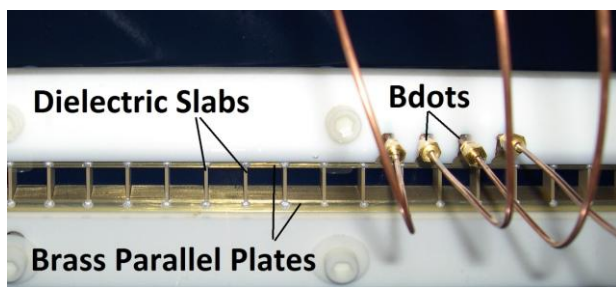


Figure 6. Experimental NLTL.

## Experimental Data

The experiment was run with pulser output voltages ranging from 4-43 kV. At voltages below 4 kV, the line does not sharpen the waveform since  $dC/dV$  is positive, Figure 2. The evolution of a 41 kV input pulse is shown in Figure 7. Above  $\sim 0.5$  kA,

where  $dC/dV$  changes sign from positive to negative, an electromagnetic shockwave is formed with a risetime of approximately 3 ns. Due to the high loss present in the PMN38 dielectric material strong oscillations were never formed as the shockwave propagated down the NLTL. There is some evidence of oscillations after the peak on the traces from Bdots 13-16, however the depth of these oscillations was very small. This behavior was expected based on the simulation shown in Figure 5 where the shockwave forms; however, with a  $2\ \Omega$  ESR oscillations do not develop.

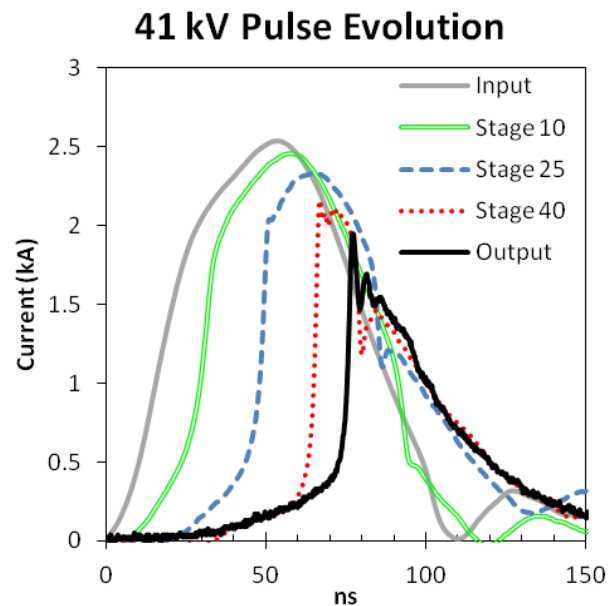


Figure 7. Traces showing the evolution of a 41kV input pulse.

The velocity of the pulse down the line is calculated by measuring the time between adjacent sets of Bdots. The velocity of 1.5 kA part of the pulse is calculated to be  $0.051 \pm 0.002c$ . Since the velocity of a signal on the transmission line is given by  $v = (LC)^{-1/2}$ , where  $L$  and  $C$  are per unit length and the inductance is known, the velocity is used to determine the capacitance. For the 1.5 kA current with the velocity determined above and the inductance of  $13\ \text{nH}/1.676\ \text{cm}$  the capacitance per stage is  $92 \pm 4\ \text{pF}$ . For a 4 kV input pulse the 0.1 kA velocity is  $0.035 \pm 0.002c$ . This results in a capacitance of  $196 \pm 11\ \text{pF}$ . The 4 kV capacitance value is expected based on the functional form of the capacitance shown in Figure 2, however, it is expected that the capacitance for the 41 kV input pulse would be  $< 50\ \text{pF}$  based on Figure 2, the difference between the measured and expected may

be due to the high loss within the material. The capacitance values are used to determine the impedance at low and high voltages using  $Z = (L/C)^{1/2}$ . The impedances are 8.1  $\Omega$  and 11.9  $\Omega$  for the 4 kV and 41 kV input pulses respectively. An additional diagnostic for the impedance is the presence of the capacitance feature at 4 kV where  $dC/dV$  changes sign. The shock in Figure 7 begins at  $\sim 0.5$  kA, which gives 4 kV/0.5 kA = 8  $\Omega$ .

## Conclusions

A nonlinear dielectric-based nonlinear transmission line was constructed and tested. The NLTL was modeled in a circuit simulation code using the experimentally measured form of the nonlinear capacitance. Dielectric loss is included in the model as an equivalent series resistance derived from the measured loss tangent data. The loss included in the simulation prevents the formation of RF oscillations. The experimental line was tested at input voltages from 4-43 kV and showed the expected nonlinear behavior with waveforms showing shockwave generation as they travel down the transmission line. The waveforms from the experimental line compare qualitatively with the circuit model, showing no strong RF formation as a result of the loss in the PMN38 material. An analysis of the velocity of the waveform on the transmission line can be used to probe the nonlinearity of the dielectric material. In this case, the impedance of the line was determined using velocity to measure the capacitance of the line at low and high pulse voltages.

## References

- [1] H. Ikezi, J.S. DeGrassie, and J. Drake, "Soliton generation at 10 MW level in the very high frequency band," *Applied Physics Letters*, vol. 58, 1991, p. 986.
- [2] H. Ikezi, S.S. Wojtowicz, R.E. Waltz, and D.R. Baker, "Temporal contraction of solitons in a nonuniform transmission line," *Journal of Applied Physics*, vol. 64, Dec. 1988, pp. 6836-6838.
- [3] TRS Technologies, Inc., <http://www.trstechnologies.com/>.
- [4] Linear Technology- <http://www.linear.com/designtools/software/ltspice.jsp>.